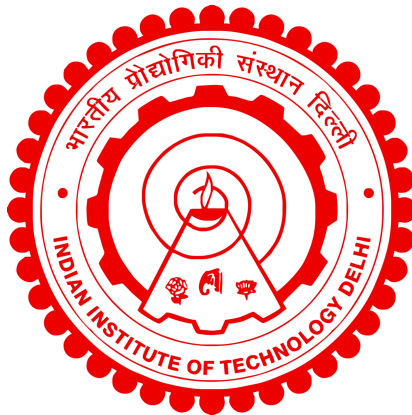


**DEVELOPMENT OF TiNbMoMnFe BULK
MULTI-PRINCIPAL ELEMENT ALLOYS AND
THEIR COATINGS**

ABHIJITH N V



**CENTRE FOR AUTOMOTIVE RESEARCH AND
TRIBOLOGY**

INDIAN INSTITUTE OF TECHNOLOGY DELHI

MAY 2025

© Indian Institute of Technology Delhi (IITD), New Delhi, 2025

**DEVELOPMENT OF TiNbMoMnFe BULK
MULTI-PRINCIPAL ELEMENT ALLOYS AND
THEIR COATINGS**

by

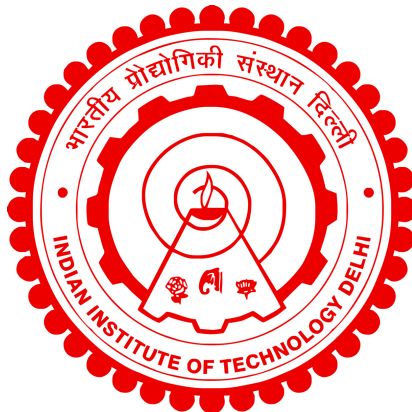
ABHIJITH N V

**CENTRE FOR AUTOMOTIVE RESEARCH AND
TRIBOLOGY**

submitted

in fulfillment of the requirements of the degree of Doctor of Philosophy

to the



INDIAN INSTITUTE OF TECHNOLOGY DELHI

MAY 2025

Dedicated to my parents

Mr.Venugopala Pillai .R and Mrs.Leelamony .S

Certificate

This is to certify that the thesis entitled “**Development of TiNbMoMnFe bulk multi-principal element alloys and their coatings**”, submitted by **Mr. Abhijith N V** to the Indian Institute of Technology Delhi, for the award of the degree of **Doctor of Philosophy** in May 2025, is a record of the original, bonafide research work carried out by him under my supervision and guidance. The thesis has reached standards that meet the requirements of the regulations related to the award of the degree.

The results contained in this thesis have not been submitted in part or in full to any other University or Institute for the award of any degree or diploma to the best of our knowledge.



Dr. Deepak Kumar

Professor and Head

Centre for Automotive Research and Tribology
Indian Institute of Technology Delhi

Place : New Delhi

Date : 21-05-2025

Acknowledgements

Firstly, I wish to express my gratitude to the divine for instilling a sense of self-confidence in me and for bestowing blessings upon me during this journey. I am profoundly grateful to my parents, Venugopala Pillai .R, and Leelamony .S, my sister, Dr. Anagha .L .V, and my brother-in-law, Vignesh R P Nair, for their unwavering support during this journey.

I wish to convey my sincere thanks to my supervisor, Prof. Deepak Kumar, for his valuable guidance and unwavering encouragement in my research work. The distinctive and stimulating viewpoints on research and beyond fostered a scientific mindset in me and enhanced my confidence to confront any challenges throughout this journey.

I express profound thanks to my SRC members (Prof. S. Fatima, Prof. H. Kanchwala, and Prof. R. K. Pandey) for providing constructive criticism throughout the semester's progress presentations. I convey sincere thanks to Prof. D. Kalyanasundaram, the Nano Research Facility (NRF), and the Central Research Facility (CRF) of the Indian Institute of Technology Delhi for their experimental support and prompt assistance.

I extend my appreciation to our research group, especially Dr. Bharat Kumar, Dr. Abhijit Pattnayak, Ms. Gazal Gupta, Mr. Arun G, and Mr. Sedhuraman E; without their help and support, I could not have completed my journey.

I would like to seize this opportunity to convey my gratefulness to some special persons, including Dr. Rismaya Kumar Mishra, Mr. Jonty Mago, and Mrs. Vandana, as well as my college friends Mr. Eby Jose and Mr. Ebin Mathew, who have become indispensable contributors to my Ph.D. journey by offering emotional, and mental support throughout this endeavor. Also, I wish to thank other colleagues, Mr. Subhakar Mangam and Mr. Junaid Syed, for their experimental support.

I convey my heartfelt gratitude to the CART personnel, Mr. Shripal Singh, Mr. Lokesh, Mr. Ved Singh, Mr. Hitesh, and Mr. Avtar Singh, for their assistance in office and lab work.

I am also grateful to our seniors, Dr. Sanjeet Kumar, Dr. Harprabhjot Singh, Dr. A.P.S. Lodhi, Dr. Avi Gupta, and Dr. Ankit Saxena, for their assistance and support.

Lastly, the most significant person in my life is my M. Tech supervisor, Prof. Sudeep.

U, who consistently encouraged me to pursue a career in scientific research and offered consistent support.

Much obliged, and may God keep you safe.

Sincerely,

A handwritten signature in blue ink, appearing to read 'Abhijith', with a long horizontal flourish extending to the left.

Abhijith N V

Abstract

Steel is extensively used in many industries, including automotive, petrochemical, food processing, biomedical, and aerospace, due to its cost-effectiveness, strength, hardness, biocompatibility, wear and corrosion resistance characteristics. However, it has limitations in extreme environments. Austenitic stainless steels, like SS304, are preferred in such extreme environments, but they degrade under intense corrosive and wear conditions. Hence, these surface/sub-surface degradations of SS304 steel can be eliminated by developing a new novel material. Nowadays, a novel category of alloys known as Multi-principal Element Alloys (MPEAs) has garnered significant interest from the scientific community owing to their multifunctional features. This study focuses on developing a novel TiNbMoMnFe-based MPEA using bulk fabrication and surface coating techniques. The performance of the developed MPEA and the coating are benchmarked with the responses of the SS304 steel.

The present research has been classified into three sections: (i) the development of bulk MPEA using microwave sintering, (ii) the development of MPEA coating using the High-velocity oxy-fuel (HVOF) thermal spray process, and (iii) exploring the effect of heat treatment on HVOF-sprayed MPEA coating properties. Further, the metallurgical (XRD, FESEM, Raman, XPS, etc.), Mechanical (Hardness), Physical (Density, Porosity, Surface wettability), Tribological (Friction, Wear), and Electrochemical (Corrosion) characteristics of the bulk MPEA, MPEA coating, and heat-treated MPEA coating were studied and established the role of microstructural changes on their superior properties.

Initially, the TiNbMoMnFe-based bulk MPEA was fabricated using the microwave sintering-assisted powder metallurgy technique. The MPEA powder was initially synthesized using a mechanical alloying technique. The optimal composition of the alloyed powder was further compacted into green pellets and then microwave-sintered at different temperatures. The exact single phase (BCC: TiNbMoMnFe) MPEA evolved at 1400 °C. While sintering at less than 1400 °C resulted in multiphase (BCC, FCC) MPEA. Thus, developed single-phase (TiNbMoMnFe) MPEA exhibited a hardness of ≈ 16 GPa and porosity of around 8%. The tribological exploration suggested that the multiphase alloys (sintered at 1100 °C - 1300 °C) are prone to adhesive wear followed by oxidative wear. Due to high hardness, the

single-phase MPEA underwent minimal plastic deformation and some surface abrasion. This also resulted in the exposure of nascent surfaces, leading to oxidative wear. Hence, the wear resistance was increased by $\approx 54\%$. The single-phase MPEA (BCC: TiNbMoMnFe) showed excellent corrosion resistance (Corrosion rate: $\approx 99\%$ reduction for short-term exposure, $\approx 83\%$ reduction for long-term exposure) attributed to the lack of high-energy sites and the formation of a stable and continuous passive layer on the surface.

The SS304 steel-facing surface/sub-surface degradations can be projected by developing the MPEA coating. The TiNbMoMnFe-based MPEA coating on SS304 steel was developed using the HVOF thermal spray process. This study investigated the role of feedstock powder preparation on the overall coating performance. The MPEA coatings were developed by preparing the feedstock powder at different time scales, 5 h, 10 h, and 15 h, respectively. Among them, the 15 h milled MPEA coating exhibited a very dense and homogeneous structure with low porosity ($\approx 1\%$), superior surface finish ($R_a \approx 2.57 \mu\text{m}$), and hardness ($\approx 13 \text{ GPa}$). Tribological studies under dry sliding conditions revealed that the 15 h milled MPEA coating was highly wear-resistant compared to other coatings (86% reduction). For long-term exposure to simulated body fluid (SBF), the MPEA coating showed much-improved anticorrosion performance (corrosion rate reduced by $\approx 98\%$). The dual protective mechanism involved the formation of a TiNbMo-rich passivating layer and apatite deposition on the surface during long-term exposure. Long-term exposure to NaCl medium, 15 h MPEA coating recorded a $\approx 99.5\%$ reduction in corrosion rate after 5 weeks. The protective mechanism was associated with the formation of a TiNbMo-rich passivating layer. However, the SS304 substrate was prone to severe corrosion. The erosion studies suggested that the failure mode was ductile. The 15 h milled MPEA coating showed an $\approx 88\%$ reduction in erosion rate at a 30° impingement angle.

The 15 h milled MPEA coating was further heat-treated at 700°C , 900°C , and 1100°C , and the effect of heat treatment on the mechanical, metallurgical, corrosion, and tribological properties was studied. Heat treatment made the coating denser, more compact, and less porous. Upon heat treatment, the single-phase BCC structured as-sprayed MPEA coating transformed to dual-phase (BCC and FCC) MPEAs, and the presence of the FCC phase dominated over the BCC phase when heat-treated at 1100°C . The 900°C heat-treated coating showed the highest nano and scratch

hardness due to the dual-phase behavior, and hardness started degrading after 900 °C. Also, the 900 °C heat-treated coating had excellent wear resistance; the major wear mechanism was abrasive wear followed by oxidative wear. Similarly, the 900 °C heat-treated MPEA coating had the highest corrosion resistance ($\approx 92\%$ reduction). Hence, the particular composition is not recommended for heat treatment beyond 900 °C.

सारांश

इस्पात का उपयोग कई उद्योगों में किया जाता है, जिसमें ऑटोमोटिव, पेट्रोकेमिकल, फूड प्रोसेसिंग, बायोमेडिकल और एयरोस्पेस शामिल हैं, इसकी लागत-प्रभावशीलता, शक्ति, कठोरता, जैव-रासायनिकता, घिसाव और संक्षारण प्रतिरोध विशेषताओं के कारण। हालांकि, इसकी चरम वातावरण में सीमाएं हैं। एसएस३०४ जैसे ऑस्टेनिटिक स्टेनलेस इस्पात को ऐसे चरम वातावरण में पसंद किया जाता है, लेकिन वे तीव्र संक्षारक और घिसाव की स्थिति में खराब हो जाते हैं। इसलिए, एसएस३०४ इस्पात की इन सतह/उप-सतह गिरावट को एक नवीन सामग्री विकसित करके समाप्त किया जा सकता है। आजकल, मल्टी-प्रिंसिपल एलिमेंट मिश्र धातु (एम.पी.ई.ए) के रूप में जाने वाले मिश्र धातुओं की एक नवीन श्रेणी ने वैज्ञानिक समुदाय से उनकी बहुक्रियाशील विशेषताओं के कारण महत्वपूर्ण रुचि प्राप्त की है। यह अध्ययन बल्क उत्पादन और उपरितल आवरण तकनीकों का उपयोग करके एक नवीन टीआई एनबी एमओ एमएन फ़े-आधारित एमपीईए विकसित करने पर केंद्रित है। विकसित एम.पी.ई.ए और उनके आवरण के प्रदर्शन को एसएस३०४ इस्पात की प्रतिक्रियाओं के साथ तुलना किया गया है। वर्तमान अनुसंधान को तीन वर्गों में वर्गीकृत किया गया है: (i) माइक्रोवेव सेंट्रिंग का उपयोग करते हुए बल्क एम.पी.ई.ए का विकास, (ii) हाई-वेलोसिटी ऑक्सी-फ्यूल (एच.वी.ओ.एफ.) थर्मल स्प्रे प्रक्रिया का उपयोग करके एम.पी.ई.ए आवरण का विकास, और (iii) छिड़काव किए गए एम.पी.ई.ए आवरण गुणों पर ऊष्मा-उपचारित के प्रभाव की खोज। इसके अलावा, धातुकर्म (एक्स.आर.डी, एफ.ई.एस.ई.एम, रमन, एक्स.पी.एस, आदि), यांत्रिक (कठोरता), भौतिक (घनत्व, सरंध्रता, सतह आर्द्रशीलता), ट्राइबोलॉजिकल (घर्षण, घिसाव) और बल्क एम.पी.ई.ए, एम.पी.ई.ए आवरण, और ऊष्मा-उपचारित एम.पी.ई.ए आवरण की विशेषताओं का अध्ययन किया गया और उनके बेहतर गुणों पर उनकी सूक्ष्म संरचना में परिवर्तन की भूमिका बनाई गयी। प्रारंभ में, टीआई एनबी एमओ एमएन फ़े-आधारित ठोस एम.पी.ई.ए को माइक्रोवेव सेंट्रिंग-सहायता प्राप्त पाउडर धातुकर्म तकनीक का उपयोग करके निर्मित किया गया था। एम.पी.ई.ए पाउडर को शुरू में एक यांत्रिक मिश्रधातु तकनीक का उपयोग करके संश्लेषित किया गया था। मिश्रित पाउडर की इष्टतम संरचना को आगे हरे छरों में संकुचित किया गया और फिर विभिन्न तापमानों पर माइक्रोवेव-सेंटर किया गया। इस्पात एकल चरण (बी सी सी: टीआई एनबी एमओ एमएन फ़े) एम.पी.ई.ए १४०० डिग्री सेल्सियस पर विकसित हुआ। जबकि १४०० डिग्री सेल्सियस से कम पर सेंट्रिंग के परिणामस्वरूप बहु चरण (बीसीसी, एफसीसी) एमपीईए होता है। इस प्रकार, विकसित एकल-चरण (टीआई एनबी एमओ एमएन फ़े) एम.पी.ई.ए ने \approx १६ जीपीए की कठोरता और लगभग ८% की सरंध्रता प्रदर्शित की। ट्राइबोलॉजिकल अन्वेषण ने सुझाव दिया कि मल्टीफ़ेज़ मिश्र धातु (११०० डिग्री सेल्सियस - १३०० डिग्री सेल्सियस पर सेंटर किए गए) चिपकने वाले पहनने के बाद ऑक्सीडेटिव पहनने के लिए प्रवण होते हैं। उच्च कठोरता के कारण, एकल-चरण एम.पी.ई.ए में न्यूनतम प्लास्टिक विरूपण और कुछ सतह घर्षण हुआ। इसके परिणामस्वरूप नवजात सतहें भी उजागर हो गईं, जिससे ऑक्सीकरण घिसाव हुआ। इसलिए, पहनने के प्रतिरोध में \approx ५४% की वृद्धि हुई। एकल-चरण एम.पी.ई.ए (बी सी सी: टीआई एनबी एमओ एमएन फ़े) ने उत्कृष्ट संक्षारण प्रतिरोध दिखाया (संक्षारण दर: अल्पकालिक अनावरण के लिए ९९% की कमी, दीर्घकालिक अनावरण के लिए लगभग ८३% की कमी) उच्च-ऊर्जा स्थान की कमी और सतह पर एक स्थिर और निरंतर निष्क्रिय परत के गठन के लिए जिम्मेदार है।

एम.पी.ई.ए आवरण विकसित करके एसएस३०४ इस्पात को सतह/उप-सतह क्षरण का अनुमान लगाया जा सकता है। एसएस३०४ इस्पात पर (टीआई एनबी एमओ एमएन फ्रे)-आधारित एम.पी.ई.ए आवरण एच.वी.ओ.एफ थर्मल स्प्रे प्रक्रिया का उपयोग करके विकसित की गई थी। इस अध्ययन ने समग्र आवरण प्रदर्शन पर निवेश सामग्री तैयार करने की भूमिका की जांच की। एम.पी.ई.ए आवरण को निवेश सामग्री को क्रमशः ५ घंटे, १० घंटे और १५ घंटे के अलग-अलग समय के पैमाने पर तैयार करके विकसित किया गया था। उनमें से, १५ घंटे मिल्ड एम.पी.ई.ए आवरण ने कम सरंध्रता ($\approx 1\%$), बेहतर सतह खत्म (≈ 2.57 माइक्रो मीटर), और कठोरता (≈ 13 जीपीए) के साथ बहुत घनी और सजातीय संरचना प्रदर्शित की। ड्राई स्लाइडिंग स्थितियों के तहत ट्राइबोलॉजिकल अध्ययनों से पता चला कि १५ घंटे मिल्ड एम.पी.ई.ए आवरण अन्य आवरण (८६% कमी) की तुलना में अत्यधिक घिसाव के लिए प्रतिरोधी थी। सिम्युलेटेड शरीर द्रव (एसबीएफ) के लंबे समय तक संपर्क के लिए, एम.पी.ई.ए आवरण ने एंटीकोर्सॉशन प्रदर्शन में काफी सुधार दिखाया (जंग दर $\approx 98\%$ कम हो गई)। दोहरे सुरक्षात्मक तंत्र में दीर्घकालिक अनावरण के दौरान सतह पर टीआई एनबी एमओ-समृद्ध निष्क्रिय परत और एपेटाइट जमाव का निर्माण शामिल था। एनएसीएल माध्यम, १५ घंटे एम.पी.ई.ए आवरण के लंबे समय तक संपर्क में रहने से ५ सप्ताह के बाद संक्षारण दर में $\approx 99.5\%$ की कमी दर्ज की गई। सुरक्षात्मक तंत्र एक टीआई एनबी एमओ-समृद्ध निष्क्रिय परत के गठन से जुड़ा था। हालाँकि, एसएस३०४ क्रियाधार में गंभीर क्षरण का खतरा था। क्षरण अध्ययन ने सुझाव दिया कि विफलता मोड लचीला था। १५ घंटे मिल्ड एम.पी.ई.ए आवरण ने 30° टकराव कोण पर क्षरण दर में $\approx 88\%$ की कमी दिखाई।

१५ घंटे मिल्ड एम.पी.ई.ए आवरण को ७०० डिग्री सेल्सियस, ९०० डिग्री सेल्सियस और ११०० डिग्री सेल्सियस पर आगे गर्मी-उपचार किया गया और यांत्रिक, धातुकर्म, संक्षारण और ट्राइबोलॉजिकल गुणों पर ताप उपचार के प्रभाव का अध्ययन किया गया। ताप उपचार ने आवरण को सघन, अधिक सघन और कम छिद्रपूर्ण बना दिया। ताप उपचार पर, एकल-चरण बीसीसी संरचित स्थिति एम.पी.ई.ए आवरण दोहरे चरण (बीसीसी और एफसीसी) एम.पी.ई.ए में बदल जाती है, और जब ११०० डिग्री सेल्सियस पर ताप का इलाज किया जाता है तो एफसीसी चरण की उपस्थिति बीसीसी चरण पर हावी हो जाती है। ९०० डिग्री सेल्सियस ताप-उपचारित आवरण ने दोहरे चरण के व्यवहार के कारण उच्चतम नैनो और खरोच कठोरता दिखाई, और ९०० डिग्री सेल्सियस के बाद कठोरता कम होने लगी। इसके अलावा, ९०० डिग्री सेल्सियस ताप-उपचारित आवरण में उत्कृष्ट घिसाव का प्रतिरोध था; प्रमुख घिसाव तंत्र अपघर्षक घिसाव और उसके बाद ऑक्सीकरण घिसाव था। इसी प्रकार, ९०० डिग्री सेल्सियस ताप-उपचारित एम.पी.ई.ए आवरण में उच्चतम संक्षारण प्रतिरोध ($\approx 92\%$ कमी) था। इसलिए, ९०० डिग्री सेल्सियस से अधिक ताप उपचार के लिए विशेष संरचना की अनुशंसा नहीं की जाती है।

Contents

Certificate	i
Acknowledgements	ii
Abstract	iv
सारांश	vii
Contents	ix
List of Figures	xiii
List of Tables	xviii
Abbreviations	xx
1 Introduction and literature survey	1
1.1 Introduction	1
1.2 Potential application	2
1.3 Microwave sintering	4
1.4 Surface coating	6
1.5 High-velocity oxy-fuel (HVOF) process	7
1.6 Multi-principal element alloys (MPEAs)	8
1.7 Literature review	11
1.7.1 MPEAs and their Compositions	11
1.7.2 Bulk MPEAs and microwave sintering	14
1.7.3 Development of MPEA Coatings	17
1.8 Motivation	18
1.9 Problem formulation	19
1.9.1 Problem identification	19

1.9.2	Problem definition	20
1.9.3	Research objectives	22
1.9.4	Approach	22
1.10	Thesis outline	23
1.10.1	Chapter 1 Introduction and Literature Survey	24
1.10.2	Chapter 2 Materials and methods	24
1.10.3	Chapter 3 Development of bulk MPEA using microwave sintering	25
1.10.4	Chapter 4 Development of MPEA coating using the HVOF thermal spray process	26
1.10.5	Chapter 5 Effect of heat treatment on MPEA coating characteristics	26
1.10.6	Chapter 6 Conclusions and Future Scope	27
2	Materials and methods	29
2.1	Powder preparation	30
2.2	Microwave sintering	30
2.3	Substrate preparation and coating deposition	31
2.4	Heat treatment of coated samples	34
2.5	Physical characterization	34
2.5.1	Surface roughness	34
2.5.2	Density	34
2.5.3	Wettability analysis	35
2.6	Mechanical characterization	35
2.6.1	Micro hardness	35
2.6.2	Nano hardness	35
2.6.3	Scratch hardness	36
2.7	Microstructural and Metallurgical characterization	37
2.7.1	Scanning electron microscopy (SEM)	37
2.7.2	Field emission scanning electron microscopy (FESEM)	37
2.7.3	Energy dispersive X-ray spectroscopy (EDS)	38
2.7.4	X-ray photoelectron spectroscopy (XPS)	38
2.7.5	X-ray diffraction (XRD)	38
2.7.6	Raman spectroscopy	39
2.8	Electrochemical characterization	39
2.8.1	Corrosion response	39
2.8.2	Fourier transform-infrared (FTIR) spectroscopy	40
2.8.3	pH distribution	40
2.9	Tribological characterization	40
2.10	Erosion characterization	41
3	Development of bulk MPEA using microwave sintering process	43

3.1	Thermodynamic aspects of MPEA	44
3.2	Powder characterization	44
3.3	Microstructural and metallurgical characterization	49
3.4	Mechanical and physical characterization	54
3.4.1	Hardness	55
3.4.2	Density and porosity	55
3.4.3	Wettability analysis	56
3.5	Tribological characterization	57
3.5.1	Friction	57
3.5.2	Wear	59
3.6	Corrosion characterization	63
3.6.1	Short-term corrosion in NaCl medium	63
3.6.2	Long-term corrosion in NaCl medium	66
3.6.3	Corrosion mechanism	68
3.7	Summary	73
4	Development of MPEA coating using the HVOF thermal spray process	75
4.1	Thermodynamic aspects of MPEA Coating	76
4.2	Microstructural and metallurgical characterization	78
4.3	Mechanical and physical characterization	82
4.3.1	Hardness	82
4.3.2	Density and porosity	85
4.3.3	Surface roughness	86
4.3.4	Surface wettability analysis	86
4.3.5	Scratch resistance	88
4.4	Tribological characterization	89
4.4.1	Dry sliding condition	89
4.4.1.1	Friction	89
4.4.1.2	Wear	91
4.4.2	Lubricated sliding condition	97
4.4.2.1	Friction	97
4.4.2.2	Wear	98
4.5	Corrosion characteristics	100
4.5.1	NaCl Medium	100
4.5.1.1	Short-term exposure	100
4.5.1.2	Long-term exposure	104
4.5.1.3	Corrosion mechanism	109
4.5.2	SBF Medium	111
4.5.2.1	Long-term exposure	112
4.5.2.2	Corrosion mechanism	117
4.6	Erosion characteristics	122

4.7	Summary	125
5	Effect of heat treatment on MPEA coating characteristics	127
5.1	Microstructural and metallurgical characterization	128
5.2	Mechanical and physical characterization	130
5.2.1	Porosity and density	130
5.2.2	Nano hardness	131
5.2.3	Scratch hardness	132
5.2.4	Wettability analysis	134
5.3	Tribological characteristics	135
5.3.1	Friction	135
5.3.2	Wear	136
5.4	Corrosion characteristics	139
5.5	Summary	142
6	Conclusions and future scope	145
6.1	Conclusions	146
6.2	Future scope	148
	References	151
	List of Publications	175
	Brief biography	178

List of Figures

1.1	World steel production statistics from 2000 to 2024 (million tonnes) .	2
1.2	Schematic representation of mineral mixing plant	3
1.3	Possible solution to the surface and sub-surface degradations of SS304 steel	4
1.4	Classification of bulk alloys development techniques	5
1.5	Schematic representation of the microwave sintering process	6
1.6	Schematic diagram showing the working principle of the HVOF thermal spray process	8
1.7	Schematic representation of BCC Lattice of (a) pure metal and (b) multi-component alloy	10
1.8	History of MPEAs developments	13
1.9	Schematic representation of conventional and microwave sintering process	15
1.10	Percentage-wise distribution for total cost of corrosion and material loss	19
1.11	Schematic representation of the problem formulation and systematic approach used for the development of bulk MPEAs and their coating	23
2.1	Sintering flow diagram for 1400 °C, 1300 °C, 1200 °C, and 1100 °C sintered pellets	31
2.2	3D optical micrograph of (a) polished and (b) grit-blasted SS304 substrates	32
2.3	Schematic of the MPEA coating development using HVOF thermal spray process	33
2.4	Schematic illustration of Vickers hardness measurement	36
2.5	Schematic illustration of scratch hardness measurement	37
3.1	SEM micrograph of (a) 0 h, (b) 5 h, (c) 10 h, and (d) 15 h milled TiNbMoMnFe metallic powders and (e-j) corresponding EDS mapping of 15 h milled powder	46
3.2	SEM and EDS micrograph of 15 h milled MPEA powder: (a_1 , a_2) microalloying and (b_1 , b_2) agglomeration, respectively	47
3.3	Schematic representation of MPEA formation during high energy ball milling	47

3.4	X-ray diffraction spectra of 0h, 5h, 10h, and 15h milled powders . . .	49
3.5	FESEM-BSE micrograph of (a) 1100 °C, (b) 1200 °C, (c) 1300 °C, and (d) 1400 °C sintered MPEA pellets	50
3.6	XRD pattern of pellets sintered at 1100 °C, 1200 °C, 1300 °C, and 1400 °C, respectively	52
3.7	Schematic representation of (a-d) microstructural changes during the sintering process and (e-g) diffusion mechanism	54
3.8	Vickers hardness indentation marks of (a)1100 °C, (b)1200 °C, (c) 1300 °C, and (d) 1400 °C sintered MPEA pellets.	55
3.9	Density and porosity distribution in MPEA pellets sintered at 1100 °C, 1200 °C, 1300 °C, and 1400 °C	56
3.10	Wettability analysis on MPEA pellets sintered at 1100 °C, 1200 °C, 1300 °C, and 1400 °C.	57
3.11	The (a) frictional response and (b) wear rate of the sintered pellets and 3D optical micrograph of the wear scar on MPEA pellets sintered at different temperatures (c) 1100 °C, (d) 1200 °C, (e) 1300 °C, and (f) 1400 °C and (g) the corresponding depth profile of the same . . .	58
3.12	FESEM micrograph of the worn surface of MPEA pellets sintered at (a) 1100 °C, (b) 1200 °C, (c) 1300 °C, and (d)1400 °C and (e,f) Raman spectra and EDS analysis of the worn surface	61
3.13	Schematic representation of different stages of wear	63
3.14	Short-term corrosion response of various sintered pellets represented in terms of (a) Tafel plot (b) Nyquist plot (c) Bode plot and (d) equivalent electrical circuit	65
3.15	Long-term corrosion response of the 1400 °C sintered MPEA pellet represented in terms of (a) Tafel plot (b) Nyquist plot (c) Bode plot, and (d) equivalent electrical circuit and (e,f) FTIR spectra and pH variation of the electrolyte after 5 weeks, respectively	67
3.16	Schematic representation of possible corrosion mechanism	70
3.17	XPS analysis of (a-e) bare sample and (f-j) passive layer in the corroded area	71
4.1	BSE-FESEM cross-sectional micrograph of (a) 5 h, (b) 10 h, and (c) 15 h milled MPEA coatings	79
4.2	EDS-assisted elemental mapping of 15 h milled MPEA coating with Ti, Nb, Mo, Mn, and Fe elements	80
4.3	FESEM micrograph of (a) 15h milled MPEA coating and (b) magnified view in BSE mode; Point B refers to Phase 1, and point A refers to Phase 2	80
4.4	X-ray diffraction pattern of 5h, 10h and 15h milled MPEA coatings .	82
4.5	Vicker indentation images of (a) 5 h, (b)10 h, and (c) 15 h milled coating surfaces	83

4.6	Nanoindentation (a) load vs. displacement curve and (b) hardness, elastic modulus values of the SS304 substrate and 5 h, 10 h, and 15 h milled coatings	83
4.7	Variation of hardness and elastic modulus along the interface of 15 h milled MPEA coating	84
4.8	Variation of porosity and density in different MPEA coatings	85
4.9	3D surface roughness profile of (a) 5 h, (b) 10 h, and (c) 15 h milled MPEA coating	87
4.10	Variation of water contact angles on bare SS304 substrate and different MPEA coatings	88
4.11	The 2D optical images of the scratch on (a) SS304 and (b) 15 h milled MPEA coating and corresponding surface profile (a_1 , b_1) of the scratch and (c_1) variation of COF values	89
4.12	Variation of COF for SS304, 5 h, 10 h, and 15 h milled coating sliding against EN31 balls	90
4.13	Representative 3D topographic images of wear scars on (a) SS304 substrate and (b) 5 h, (c) 10 h, and (d) 15 h milled powder coatings; and (e) 2D cross-sectional profile of wear scars	92
4.14	Average values of friction coefficient and wear rate for bare SS304 steel and 5 h, 10 h, and 15 h milled powder coatings	92
4.15	SEM micrographs of worn surfaces of (a) SS304, (b) 5 h, (c) 10 h, and (d) 15 h milled MPEA coatings	93
4.16	SEM micrograph (a) and EDS analysis of the tribo-layer (b) on the coating and (c-e) the mechanism of tribo-layer formation on 5 h, 10 h, and 15 h milled MPEA coatings	94
4.17	XPS analysis of the wear scar of 15 h milled MPEA coating	95
4.18	Worn surface morphology of counterpart moved against (a) SS304, (b) 5 h, (c) 10 h, and (d) 15 h milled coating and (e) EDS spectra of the same	96
4.19	Variation of COF of SS304 substrate and coating in SBF medium	97
4.20	The distribution of wear rate and COF of SS304 substrate and coating in SBF medium	98
4.21	Morphological analysis of worn surfaces: schematic representation of tribo-pair (a, b), 3D optical images of wear scar on the alumina ball sliding against (a_1) SS304 substrate, (b_1) 15 h MPEA coating, 2D optical images of wear scar on (a_2) SS304 substrate, (b_2) 15 h MPEA coating and (c) corresponding depth profile of the wear scar, and (d) Raman spectra on the worn alumina balls	100
4.22	FESEM micrograph of the worn-out area on (a) SS304 substrate, (b) 15h MPEA coating, and (b_1 - b_6) elemental mapping of the oxide layer on the coating	101

4.23	The short-term corrosion response of the various specimens represented in the form of (a) Tafel plot, (b) Nyquist plot, (c) Bode plot, and (d,e) equivalent electrical circuit for SS304 and coating, respectively	102
4.24	The long-term potentiodynamic polarization response of (a) SS304, (b) 15h coating, and (c,d) pH distribution and FTIR spectra of the electrolytes for 1 to 5 weeks	105
4.25	The long-term exposure EIS response of (a,c) SS304, (b,d) 15h coating, and (e,f) EEC for SS304 and 15h coating, respectively	107
4.26	FESEM micrograph of corrosion area on (a,b) 15h MPEA coating and (c,d) SS304 substrate during week 1 and week 5, respectively	110
4.27	Schematic illustration of possible corrosion mechanism on (a-c) SS304 substrate (d-f) 15h MPEA coating	111
4.28	The potentiodynamic polarization results of (a) SS304, (b) MPEA coating, and (c) pH variation of SBF up to 5 weeks and (d) FTIR spectra of the SBF after 5 weeks	114
4.29	EIS estimates in terms of (a) and (b) Nyquist and Bode plots for SS304, respectively. (c) and (d) Nyquist and Bode plots for MPEA coating tested in SBF up to 5 weeks, respectively.	115
4.30	The equivalent electrical circuit model for (a) SS304 substrate and (b) 15h MPEA coating	116
4.31	FESEM micrograph of the SBF exposed area on (a-c) SS304 substrate and (d-f) MPEA coating during week-1, week-3, and week-5, respectively, and (c ₁ -c ₆), (f ₁ -f ₆) are the elemental mapping of the apatite formed on SS304 substrate and MPEA coating surface after 5 weeks.	118
4.32	XPS spectra of the corroded area on (a-d) SS304 substrate and (e-j) MPEA coating after week - 5	119
4.33	Schematic representation of the mechanism for the static exposure of (a-c) bare SS304 and (d-f) MPEA-coated SS304 steel	120
4.34	FESEM micrograph of the erodent (a) AlO ₃ and (c,d) respective elemental mapping and (b) particle size distribution of the Al ₂ O ₃	122
4.35	Erosion response of SS304 substrate and 15h milled MPEA coating at different impingement angles	123
4.36	FESEM micrograph of the eroded surfaces of (a-c) 15h milled MPEA coating and (d-f) SS304 substrate at 30°, 60° and 90° impingement angles and (g-i) respective erosion mechanism	124
5.1	Cross-sectional FESEM micrograph of (a) as-sprayed, (b) 700 °C, (c) 900 °C, and (d) 1100 °C heat-treated MPEA coating and (e-i) corresponding elemental mapping of the 1100 °C heat-treated coating	129
5.2	XRD spectra of as-sprayed, 700 °C, 900 °C, and 1100 °C heat treated MPEA coating	130

5.3	Porosity and density distribution of as-sprayed and various heat-treated MPEA coatings	131
5.4	Nano hardness distribution of as-sprayed and various heat-treated MPEA coatings	132
5.5	Scratch hardness distribution of as-sprayed and various heat-treated MPEA coatings	133
5.6	3D Scratch profile on (a) as-sprayed, (b) 700 °C, (c) 900 °C, and (d) 1100 °C heat-treated MPEA coating	134
5.7	Contact angle on as-sprayed and various heat-treated MPEA coatings	135
5.8	Variation of COF for as-sprayed and various heat-treated MPEA coatings	136
5.9	Wear rate variation in as-sprayed and various heat-treated MPEA coatings	137
5.10	3D optical images of the wear scar on (a) as-sprayed, (b) 700 °C, (c) 900 °C, and (d) 1100 °C heat-treated MPEA coating	137
5.11	FESEM micrograph of the wear scar on (a) as-sprayed, (b) 700°C, (c) 900 °C, and (d) 1100 °C heat-treated MPEA coating	138
5.12	The corrosion response of the various coatings represented in the form of (a) Tafel plot, (b) Nyquist plot, (c) Bode plot, and (d) equivalent electrical circuit	140
5.13	Distribution of the passive layer across the heat-treated MPEA coating	141

List of Tables

1.1	Comparison of thermal spray processes	7
2.1	HVOF coating parameters	33
2.2	Erosion test parameters	41
3.1	Thermodynamic parameters of MPEA	44
3.2	Elemental analysis of dark and white phases in different sintered MPEA pellets	51
3.3	Crystallite size and lattice strain of milled powder and sintered MPEA pellets	53
3.4	Short-term PDP parameters	64
3.5	Short-term EIS parameters	65
3.6	Long-term PDP parameters	68
3.7	Long-term EIS parameters	68
3.8	Elemental analysis of corroded area obtained from Fig. 3.16b	70
4.1	MPEA design parameters	78
4.2	Elemental analysis of the MPEA coatings and milled powders corresponding to Figure 4.1 and Figure 3.1	81
4.3	Hardness and elastic modulus values from load-displacement curve	84
4.4	Short-term potentiodynamic polarization parameters	101
4.5	Short-term EIS parameters	103
4.6	Long-term potentiodynamic polarization parameters of SS304 for 1 to 5 weeks	106
4.7	Long-term potentiodynamic polarization parameters of 15h MPEA coating for 1 to 5 weeks	106
4.8	EIS parameters of SS304 for 1 to 5 weeks	108
4.9	EIS parameters of 15h MPEA coating for 1 to 5 weeks	108
4.10	Point EDS analysis of corroded area shown in Figure 4.26	109
4.11	Potentiodynamic polarization parameters of SS304 and 15h MPEA coating in SBF for 1 to 5 weeks	113
4.12	EIS parameters achieved based on an equivalent electrical circuit model	116
5.1	Elemental analysis of as-sprayed and 1100°C heat-treated coating	129

5.2	Potentiodynamic polarization parameters	141
5.3	EIS parameters	141

Abbreviations

MPEA	M ulti P rincipal E lement A lloy
HVOF	H igh V elocity O xygen F uel
HEBM	H igh E nergy B all M illing
COF	C oefficient of F riction
HV	V ickers H ardness
HS	S cratch H ardness
EIS	E lectrochemical I mpedance S pectroscopy
EEC	E quivalent E lectrical C ircuit
PDP	P otentio D ynamic P olarization
SBF	S imulated B ody F luid
FTIR	F ourier T ransform I nfra R ed S pectroscopy
CPE	C onstant P hase E lement
SEM	S canning E lectron M icroscopy
BSE	B ack S cattered E lectron
FESEM	F ield E mission S canning E lectron M icroscopy
EDS	E nergy D ispersive S pectroscopy
XRD	X -ray D iffraction
XPS	X -ray P hoto electron S pectroscopy
BCC	B ody C entered C ubic
FCC	F ace C entered C ubic
PBR	P illing B edworth R atio